

1 **Microbial DNA on the move: sequencing based detection and analysis**
2 **of transduced DNA in pure cultures and microbial communities**
3

4 Manuel Kleiner¹, Brian Bushnell², Kenneth E. Sanderson³, Lora V. Hooper^{4,5}, Breck A. Duerkop⁶
5

6 Affiliations:

7 1: Department of Plant and Microbial Biology, North Carolina State University, Raleigh, NC, USA

8 2: Department of Energy, Joint Genome Institute, Walnut Creek, CA, USA

9 3: Department of Biological Sciences, University of Calgary, Calgary, AB, Canada

10 4: Department of Immunology, University of Texas Southwestern Medical Center, Dallas, TX, USA

11 5: Howard Hughes Medical Institute, University of Texas Southwestern Medical Center, Dallas, TX, USA

12 6: Department of Immunology and Microbiology, University of Colorado School of Medicine, Aurora,
13 CO, USA

14

15

16

17 Correspondence:

18 Manuel Kleiner – manuel_kleiner@ncsu.edu

19 Breck Duerkop – breck.duerkop@cuanschutz.edu

20 **Abstract**

21 Horizontal gene transfer (HGT) plays a central role in microbial evolution. Our understanding of the
22 mechanisms, frequency and taxonomic range of HGT in polymicrobial environments is limited, as we
23 currently rely on historical HGT events inferred from genome sequencing and studies involving cultured
24 microorganisms. We lack approaches to observe ongoing HGT in microbial communities. To address this
25 knowledge gap, we developed a DNA sequencing based “transductomics” approach that detects and
26 characterizes microbial DNA transferred via transduction. We validated our approach using model
27 systems representing a range of transduction modes and show that we can detect numerous classes of
28 transducing DNA. Additionally, we show that we can use this methodology to obtain insights into DNA
29 transduction among all major taxonomic groups of the intestinal microbiome. This work extends the
30 genomic toolkit for the broader study of mobile DNA within microbial communities and could be used to
31 understand how phenotypes spread within microbiomes.

32 Introduction

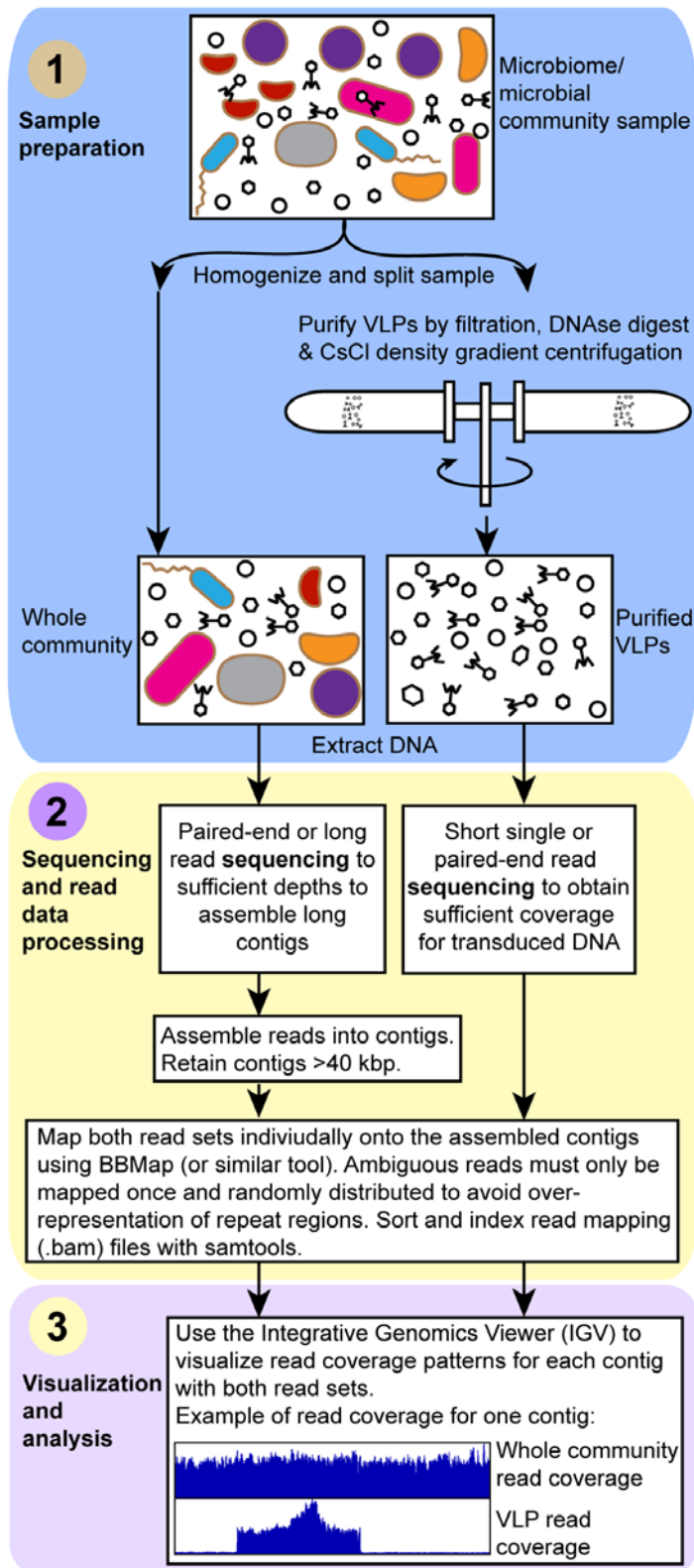
33 The importance of horizontal gene transfer (HGT) as a driver of rapid evolution and adaptation in
34 microbial communities and host-associated microbiomes has become increasingly recognized^{1,2}. Publicly
35 available genomes and metagenomes have revealed pervasive horizontally acquired genes in almost all
36 available genomes. A study of HGT in the human microbiome, for example, showed >10,000 recently
37 transferred genes in 2,235 analyzed genomes³. HGT has been implicated in the spread of antibiotic
38 resistance genes⁴, toxin and other virulence genes^{5,6}, as well as genes that enable digestion of dietary
39 compounds by microbes in the intestine⁷ and metabolic genes that augment microbial metabolism with
40 critical functions in environmental populations⁸. Despite its recognized importance, our understanding of
41 the taxonomic range, frequency and mechanisms of HGT are still limited. Most studies of HGT in
42 microbiomes rely on analysis of microbial genomes^{3,9} and as such these methods attempt to reconstruct
43 historical HGT. What we currently lack are methods that measure ongoing HGT and identify the
44 mechanism of DNA transfer. Here we present a novel method that specifically determines the sequence of
45 DNA that is transferred between cells via one of the major known pathways for DNA transfer –
46 transduction.

47 Currently, there are three major ways that genetic material is known to be exchanged between microbial
48 cells, (1) transformation – uptake of DNA by naturally competent cells, (2) conjugation – exchange of
49 genetic material (e.g. plasmids) using direct contact between donor and recipient cells, and (3)
50 transduction – transfer of genetic material by viruses or virus-like particles (VLPs)². Here we focus on
51 transduction only. There are several known types of transduction including classic specialized and
52 generalized transduction, and more recently discovered types, including gene transfer agents (GTAs),
53 lateral transduction and hijacking of bacteriophage (phage) particles by genomic islands¹⁰⁻¹². During
54 specialized transduction DNA adjacent to phage integration sites in the bacterial genomes (prophages) is
55 packaged at low frequency upon prophage excision and phage genome packaging. In generalized
56 transduction non-random pieces of the host bacterial genomic DNA or plasmids get packaged at low
57 frequency into phage particles when a lytic phage infects and replicates in a bacterial cell. This non-
58 random packaging is mediated by genomic features that resemble the packaging site (*pac* site) on the
59 phage genome, which is used by the phage particle packaging machinery as the start site phage DNA
60 packaging into the capsid¹³. GTAs are phage-like particles encoded in bacterial genomes that package
61 random pieces of the genomic DNA upon production and can transfer these pieces to other cells¹⁰. In
62 contrast to phages, GTAs do not carry the DNA content sufficient to support their reproduction in the
63 target cells. Lastly, some genomic islands, including pathogenicity islands, can hijack phages capsids in
64 an act of molecular piracy that enables their transduction^{14,15}.

65 The unifying characteristic of all types of transduction is that virus or VLPs serve as the vector for transfer
66 of genetic material between cells. Evidence so far indicates that these particles are abundant in most
67 environments and that transduction occurs with a high frequency^{16,17}. However, approaches for measuring
68 the abundance of transducing particles and transduction frequencies in microbiome samples are limited.
69 These approaches usually rely on the application of cultured phage to environmental samples^{16,17} or
70 sequencing of bacterial 16S rRNA genes from purified VLPs¹⁸. The latter approach can determine which
71 bacterial taxa's DNA is carried in a VLP. However, the approach is limited to marker genes for which
72 conserved PCR primer pairs exist and thus the majority of transduced DNA cannot be detected.

73 Here we describe an unbiased approach, termed “transductomics”, that uses DNA sequencing to identify
74 and characterize DNA originating from microbial cells that is carried in VLPs. This DNA is thus part of
75 the pool of potentially transduced DNA termed the “transductome”. Our approach is based on two
76 observations of transduced DNA in VLPs. First, transduced DNA often represents the genome of hosts
77 that are present in the same sample as the VLPs. Therefore, if DNA from a microbe is found within VLPs
78 purified from the same sample this indicates a potential transduction event. Second, unique regions of the
79 microbial host's genome are unevenly enriched in the VLPs, as most mechanisms of transduction do not
80 lead to random packaging of the host's genome. In the past, host DNA carried by VLPs may have been
81 sequenced during metagenomic sequencing of purified VLPs, but without appropriate analysis tools these
82 host derived sequences were classified as host contamination of the VLP sample rather than being
83 recognized as transduced DNA¹⁹.

84 The transductomics approach that we present requires the sequencing of both the complete microbial
85 community sample, and VLPs ultra-purified using CsCl density gradient centrifugation from the same
86 sample (Fig. 1). The VLP and complete sample sequencing reads are mapped to long genome contigs
87 assembled from the complete sample metagenome. These contigs represent both microbial and viral
88 genomes. Visualization of the read mapping coverages along the contigs comparing VLP and complete
89 metagenome read coverages reveals patterns that can be associated with host DNA transport via VLPs.
90 Below we will demonstrate this method first using pure culture models of different transducing phages
91 and other transducing particles. This is followed by the application of the approach to a murine intestinal
92 microbiome community.



93

94 **Figure 1: The “transductomics” workflow.** In the sample preparation step the sample is gently
95 homogenized and split into two subsamples. One subsample is directly used for whole community DNA
96 extraction, the other subsample is subjected to ultra-purification of virus-like particles (VLPs) using a

97 combination of filtration, DNase digest and CsCl density gradient centrifugation as previously described²⁰
98 followed by DNA extraction from the purified VLPs. Both DNA samples are sequenced to different
99 depths and potentially with different sequencing approaches, although in many cases the same sequencing
100 approach could be applied to both samples. For the whole community DNA sample, the sequencing must
101 focus on ultimately achieving assembly of long metagenomics contigs. For the VLP DNA sample, the
102 sequencing must focus on maximal read coverage, and no assembly is needed for these reads. The whole
103 community sequencing reads are assembled using a suitable assembler. Contigs smaller than 40 kbp are
104 discarded. Both the whole community and VLP sequencing reads are mapped onto the contigs >40 kbp
105 using BMap²¹ ensuring that ambiguously mapped reads are only used once and randomly assigned. To
106 find transduced regions, the contigs read coverage patterns for both whole community and VLP reads are
107 visualized using the Integrative Genomics Viewer²².

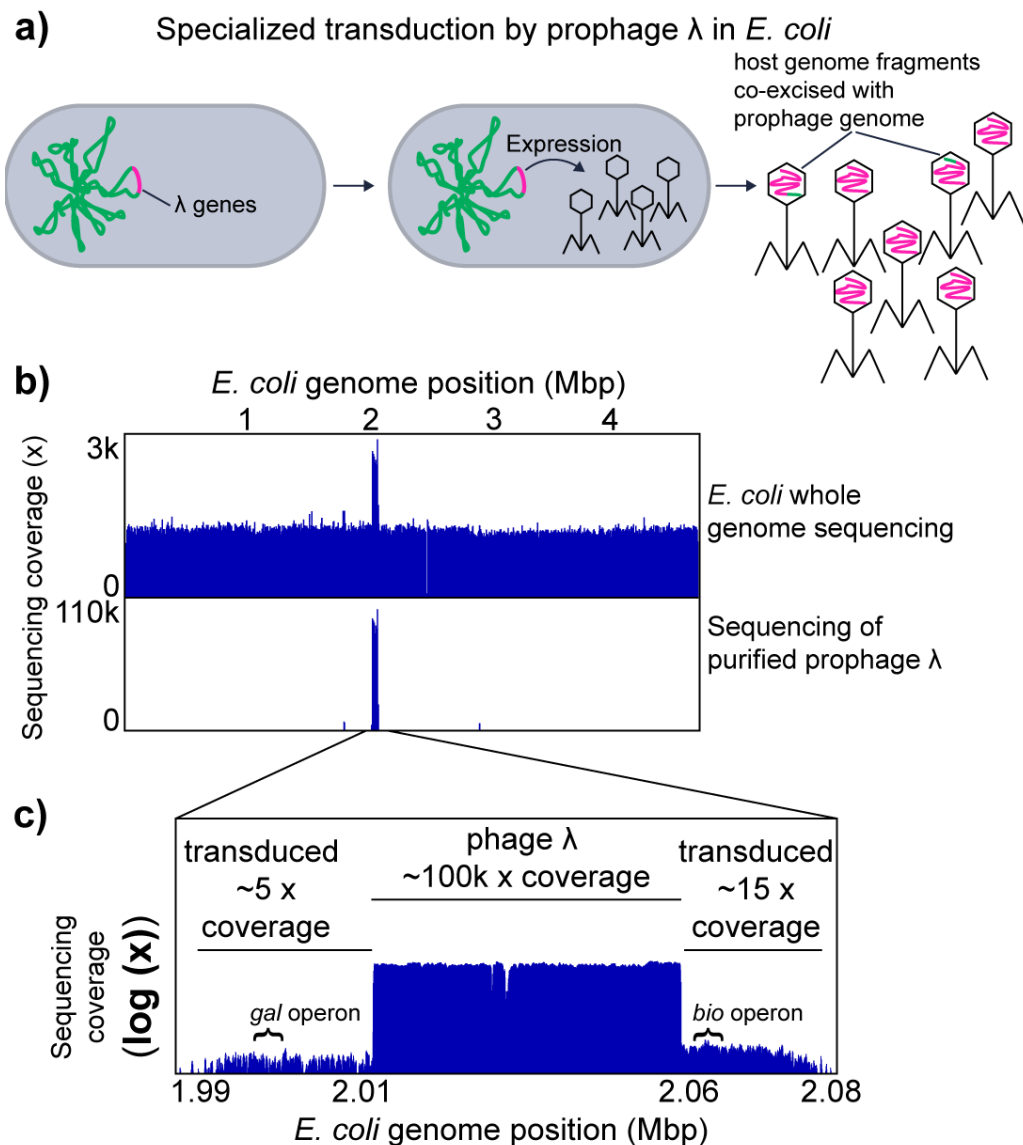
108 **Results and Discussion**

109 **Characterization of sequence coverage patterns associated with different transduction** 110 **modes in model systems**

111 **Specialized transduction by *Escherichia coli* prophage λ ²³:** We used the well-studied specialized
112 transducing bacteriophage λ to analyze the sequencing coverage patterns produced by specialized
113 transduction. In specialized transduction a prophage, which is integrated in the chromosome of the
114 bacterial host, packages host genome derived DNA with low frequency due to imprecise excision from the
115 genome upon prophage induction. Prophage λ integrates between the *gal* (galactose metabolism) and *bio*
116 (biotin metabolism) operons in the *E. coli* genome. In rare cases λ excision is imprecise and either the *gal*
117 or the *bio* operon is excised and packaged in the phage particle (Fig. 2a)²³. This packaging of adjacent *E.*
118 *coli* host derived DNA can lead to the transduction of the *bio* and the *gal* operons. Transduction of
119 recipient cells can be temporary or permanent, depending on if the DNA gets recombined into the
120 chromosome or remains as an extrachromosomal element, which is diluted out in the population during
121 cell divisions.

122 Using the transducomics approach we found that coverage of the *E. coli* genome with sequencing reads
123 derived from purified λ phage particles is almost exclusively restricted to the λ phage integration site and
124 two ~25 kbp regions on the left and right of the λ integration site (Fig. 2b and c). These flanking regions
125 with read coverage represent the regions that are transduced by λ phage as indicated by the presence of the
126 *bio* and the *gal* operons in these flanking regions (Fig. 2c). The coverage of the λ prophage region is
127 roughly 10,000 fold greater than the coverage of the flanking transduced regions indicating that only a
128 small number of phage particles actually carry transduced DNA and thus are specialized transducing
129 particles.

130 Using the *E. coli*-prophage λ model we show that specialized transduction by a prophage produces a
131 unique read coverage pattern. Furthermore, analysis of the read coverage pattern of the transduced DNA
132 region adjacent to the prophage DNA allows determination of both the size and content of the transduced
133 host genome region (~50 kbp in total in case of λ), as well as estimation of the frequency with which
134 transducing particles are produced (1:10,000 in case of λ). The number of transducing particles produced
135 based on our data is roughly 100-fold higher than previously reported values for successful transduction of
136 the *gal* operon by phage λ (1:1,000,000 successful transductions per λ particles)²⁴, which indicates that
137 only a small fraction of λ carrying host DNA ultimately leads to successful transduction.



138

139 **Figure 2:** Specialized transduction by *E. coli* prophage λ . a) Illustration of specialized transduction. The
 140 prophage λ genome is integrated into the host chromosome. Upon induction of the prophage, the prophage
 141 genome is excised and replicated. The phage structural genes are expressed, phage particles are produced
 142 and the replicated phage genome is packaged into phage heads. Ultimately the phages are released to the
 143 environment by lysis of the host cell. Imprecise excision of the prophage λ genome happens at low
 144 frequency and leads packaging of the host chromosome into phage heads. These parts of the host
 145 chromosome can be transferred to new host genomes in the process called specialized transduction. b)
 146 Genome coverage pattern associated with prophage λ induction and specialized transducing prophage λ .
 147 The upper box shows coverage patterns for whole genome sequencing reads and purified phage particle
 148 reads mapped to the *E. coli* genome. c) In the lower box, an enlargement of the purified phage read
 149 coverage for the prophage λ region is shown (log scale). The positions of the *gal* and *bio* operons, which
 150 are known to be transduced by prophage λ , are indicated²³.

151 **Generalized transduction of the *Salmonella enterica* serovar typhimurium LT2 genome by**
152 **phage P22 and the *E. coli* genome by phage P1:**

153 We used two well-studied generalized transducing bacteriophages P22 and P1 to analyze the sequencing
154 coverage patterns produced during generalized transducing events. In generalized transduction nonspecific
155 host chromosomal DNA is packaged into phage particles during lytic infection and can then be injected
156 into a new host cell (Fig. 3a). The DNA can then recombine into the host chromosome by homologous
157 recombination.

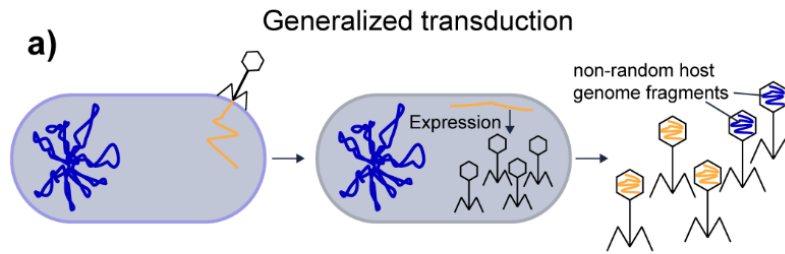
158 98.2% of the sequencing reads from purified P22 particles mapped to the P22 genome leaving 1.8% of
159 reads that map to the *S. enterica* genome. The percentage of P22 particles mapping to the *S. enterica*
160 genome corresponds to the reported percentage of 1.5% transducing P22 particles (i.e. carry host DNA)
161 previously reported²⁵. The mapped P22 derived reads covered the *S. enterica* genome unevenly, while
162 whole genome sequencing of *S. enterica* yielded even coverage (Fig. 3b). Regions of high or low P22 read
163 coverage corresponded in 23 out of 28 previously reported transduced chromosomal markers²⁶ (Fig. 3b).
164 Only one region at around 4 Mbp, for which high transduction frequencies had been reported, did not
165 show high coverage (Fig. 3b), which might be due to differences in *pac* sites within this region between
166 the *S. enterica* strain used in our study and the strain used in 1982.

167 The coverage of P22 derived reads showed a distinct pattern of peaks that rise vertically on one side and
168 decline slowly over several 100 kbp increments on the other side. We speculate that the vertical edge of
169 the peak corresponds to the location of the *pac* site at which the packaging of DNA into phage heads is
170 initiated and that the slope of the peak indicates the range of processivity of the headful packaging
171 mechanism (i.e. how many headfuls are packaged into particles before the packaging apparatus dissociates
172 from the chromosome). This speculation is based on several facts: (1) the size of host DNA carried by
173 transducing particles corresponds to the size of the P22 genome (~44 kbp)²⁷; (2) the P22 genome is
174 replicated by rolling circle replication, which produces long concatemers of P22 DNA. A specific
175 sequence on the phage DNA (*pac* site) initiates the packaging of these concatemers into phage heads using
176 a headful mechanism²⁷; (3) the packaging of phage DNA continues sequentially along the P22 genome
177 concatemer with a decreasing probability for each next headful to be encapsulated in a phage particle²⁶;
178 (4) there are five to six sequences on the *S. enterica* genome that are similar to the *pac* site, which leads to
179 packaging of *Salmonella* DNA into P22 particles upon P22 infection, albeit with much lower frequency as
180 compared to P22 DNA²⁶.

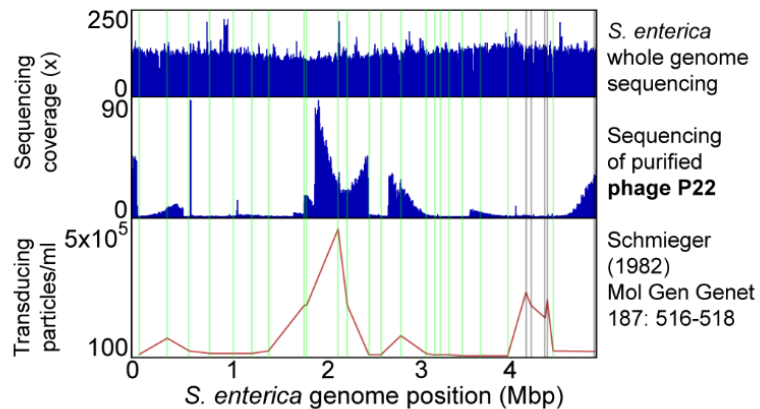
181 For *E. coli* phage P1, the majority of sequencing reads from purified P1 particles mapped to the P1
182 genome and only 4.5% of the reads mapped to the *E. coli* genome. The percentage of transducing P1
183 phages was previously reported to be 6%²⁸. We also observed that the P1 derived reads mapping to the *E.*

184 *coli* genome covered the genome unevenly. However, the pattern was less pronounced as compared to P22
185 and *S. enterica* (Fig. 3c). This low unevenness in sequencing read coverage corresponds to previous data
186 on transduction frequencies of chromosomal markers, which found a maximum transduction frequency
187 across the *E. coli* genome of 10 fold²⁹.

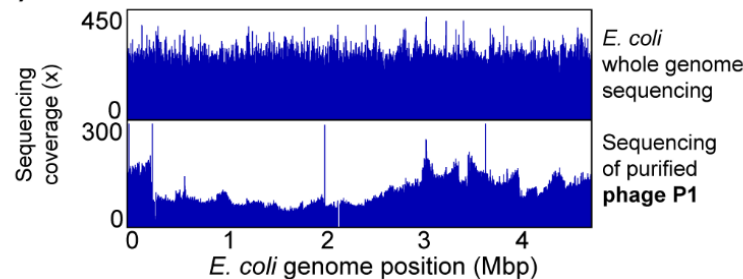
188 Sequencing host DNA carried in generalized transducing phages reveals uneven read coverage patterns
189 along the host genome indicative of transduction. These patterns vary in magnitude depending on the
190 transducing phage and they can only be observed if read coverage is analyzed along long stretches of the
191 host genome covering multiples of the length of the DNA carried by the transducing phage e.g. in case of
192 P22 44 kbp. Additionally, the patterns also provide an indication of the frequency with which different
193 regions of the host genome are transduced, as well as the locations of the *pac* sites.



b) Phage P22 in *Salmonella enterica* sv. Typhimurium LT2



c) Phage P1 in *Escherichia coli*



194

195 **Figure 3: Generalized transduction by *S. enterica* phage P22 and *E. coli* phage P1.** a) Illustration of
196 generalized transduction. Upon phage infection, the phage genome is replicated in the host cell by rolling
197 circle replication resulting in genome concatamers and phage particles are produced. The phage genome is
198 packaged into the phage head by a so called head-full packaging mechanism, which relies on the
199 recognition of a packaging (*pac*) site. The bacterial host chromosomes contain sites that resemble the *pac*
200 site and thus lead to packaging of non-random pieces of the host chromosome into phage heads. The
201 packaging happens in a processive fashion i.e. after one phage head has been filled the packaging
202 machinery continues to fill the next phage head with the remaining DNA molecule. The likelihood that the
203 packaging machinery dissociates from the molecule increases the further away from the *pac* site it gets,
204 thus leading to a decreased packaging efficiency over distance. b) *Salmonella enterica* genome coverage
205 pattern associated with generalized transduction by phage P22. Whole genome sequencing reads and
206 purified phage particle reads were mapped to the *S. enterica* genome. In the lower part transduction
207 frequencies for 28 chromosomal markers along the chromosome are shown as determined by Schmieger
208 (1982)²⁶. Vertical lines indicate the positions of the chromosomal markers in green where the transduction
209 frequency matches the read coverage, in grey where read coverage does not correspond to reported
210 transduction frequency. c) *Escherichia coli* genome coverage pattern associated with generalized
211 transduction by *E. coli* phage P1.

212 **Hijacking of helper prophage by a phage-related chromosomal island in *Enterococcus*** 213 ***faecalis* and specialized transduction by prophages**

214 Certain chromosomal islands, including pathogenicity islands and integrative plasmids, are mobilized
215 using helper phages^{14,30}. This is a form of molecular piracy in which structural proteins of the helper phage
216 are hijacked by the chromosomal island and used as a vehicle for the transfer of the island to other cells.
217 We used *E. faecalis* VE14089, which is a natural resident of the human intestine and causes opportunistic
218 infections, to study the sequencing coverage patterns produced by chromosomal island transfer by way of
219 a helper phage. *E. faecalis* VE14089 is host to a chromosomal island (EfCIV583) that uses structural
220 proteins from a helper phage (pp1) for transfer^{15,30} (Fig. 4a). *E. faecalis* VE14089 possesses five additional
221 prophage-like elements (pp2 to pp6). Some of these prophages contribute to *E. faecalis* pathogenicity and
222 confer an advantage during competition with other *E. faecalis* strains in the intestine^{15,31}.

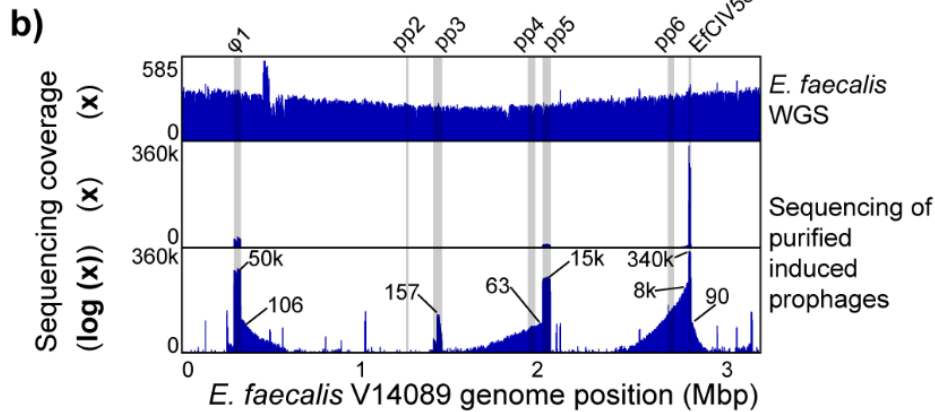
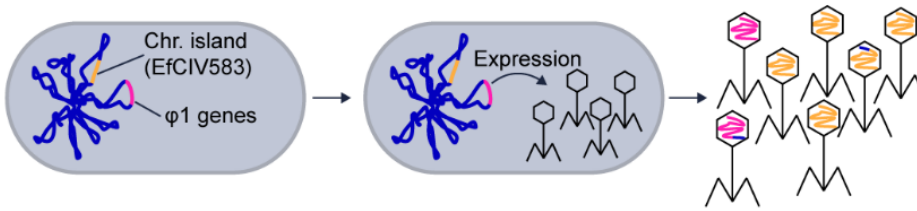
223 For pp1, pp5 and EfCIV583 we see patterns that suggest imprecise excision of the phage
224 genome/chromosomal island with a low frequency leading to specialized transduction i.e. coverage slopes
225 visible in the log-scale coverage plot. Based on the maximal coverage of the transduced regions versus the
226 coverage of the prophage regions (Fig. 4b) we estimate the maximal frequencies of transduction to be
227 1:500 for $\phi 1$, 1:240 for pp5, and 1:43 for the left side of EfCIV583 and 1:3780 for the right side of
228 EfCIV583. Read coverage differs widely between the different prophage like elements with the coverage
229 of EfCIV583 exceeding the coverage of all other elements by almost an order of magnitude (Fig. 4b). This
230 finding is in line with previous results that showed that EfCIV583 DNA is more abundant than all other
231 prophage DNA in purified VLPs from *E. faecalis* V583³¹, an isogenic strain of VE14089. Interestingly
232 pp2, pp4 and pp6 did not yield coverage peaks in the VLP fraction, which confirms previous observations
233 that these prophage elements are not excised under the conditions that we used for prophage induction¹⁵.

234 Our data also revealed that there are several additional regions in the *E. faecalis* VE14089 genome that
235 had an elevated sequencing coverage in the purified phage sample suggesting that these regions encode
236 additional elements that are transported in VLPs. These elements consist of IS-Elements that carry a
237 transposase and surprisingly the three rRNA operons. For the rRNA operons the coverage has a deep
238 valley between the 16S and the 23S rRNA gene suggesting that a specific mechanism for rRNA gene
239 transport is present or that the processed rRNAs were sequenced. We can currently think of three
240 explanations for this intriguing pattern. First, potentially ribosomes are enriched alongside the VLPs in our
241 VLP purification method. However, if this were the case we should have observed similar patterns in VLP
242 fractions of other pure culture organisms, which we did not. Second, intact ribosomes are packaged by
243 VLPs produced in *E. faecalis*. However, this leaves open the question of why the rRNA from these
244 ribosomes was amenable to sequencing by the Illumina method used, which should not enable direct
245 sequencing of RNA. Third, DNA with rRNA genes are packaged with high specificity into one or several
246 types of VLPs from *E. faecalis*.

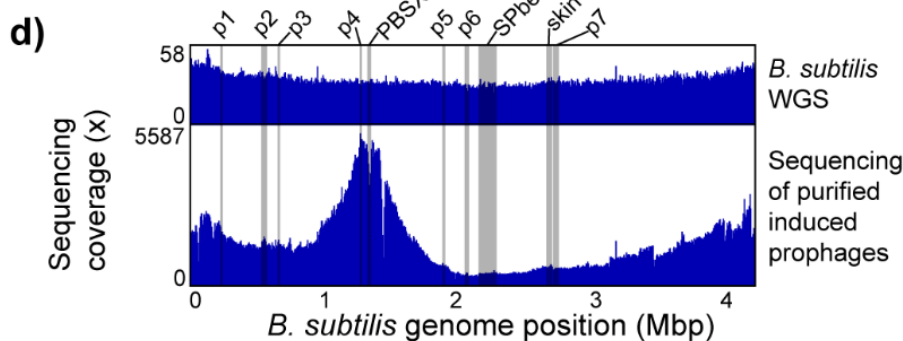
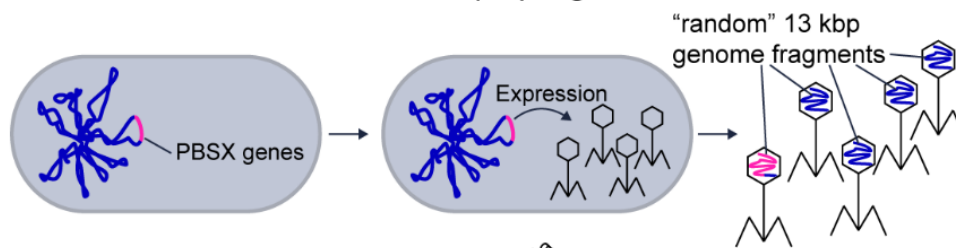
247 Our results show that the transduction of a chromosomal island by a prophage can produce a similar
248 coverage pattern as an induced prophage, indicating that chromosomal islands are easy to detect based on
249 read mapping coverage. However, they can only be distinguished from prophage by annotation of the
250 genes and genomic regions.

251

a) Specialized transduction and transduction of a chromosomal island by prophages in *E. faecalis* V14089



c) Gene transfer agent-like packaging of the *B. subtilis* chromosome by the defective prophage PBSX



252

253 **Figure 4: Other types of transduction.** a) Specialized transduction (see description for prophage λ) and
254 transduction of a chromosomal island by prophages in *E. faecalis* V14089. The chromosome of *E. faecalis*
255 contains multiple prophages including $\phi 1$ and the chromosomal island EfCIV583. Upon induction $\phi 1$ and
256 EfCIV583 are excised from the chromosome and replicated. EfCIV583 hijacks the structural proteins of
257 $\phi 1$ when they are produced and large number of phage particles that carry the EfCIV583 genome are

258 produced. b) *E. faecalis* V14089 genome coverage patterns associated with prophage induction and
259 EfCIV583 transduction. Whole genome sequencing (WGS) reads and purified VLPs were mapped to the
260 *E. faecalis* genome. The lowest part of the box shows VLP read coverage on a log scale. The small
261 numbers in this plot give x fold coverage for specific genome positions corresponding to prophages or the
262 chromosomal island EfCIV583 and the surrounding areas that are likely transduced. The positions of
263 known prophage-like elements and EfCIV583 in the *E. faecalis* genome are highlighted by grey bars. c)
264 Gene transfer agent-like packaging of the *B. subtilis* chromosome by the defective prophage PBSX. The
265 *B. subtilis* chromosome contains a variety of prophages and prophage-like elements including the
266 defective prophage PBSX³². Upon expression of the PBSX genes phage-like particles are produced, which
267 contain random 13 kbp pieces of the host chromosome³³. d) *B. subtilis* genome coverage patterns
268 associated with prophage induction. Whole genome sequencing (WGS) reads and purified prophage
269 particle reads were mapped to the *B. subtilis* genome. The positions of known prophages and prophage-
270 like elements in the *B. subtilis* genome³² are highlighted by grey bars.

271

272 **Transport of *Bacillus subtilis* genome by gene transfer agent-like element PBSX**

273 We used induced the gene transfer agent (GTA)-like element PBSX from the *B. subtilis* ATCC 6051
274 genome to study the sequencing coverage pattern produced by the supposedly randomized incorporation
275 of fragments from the whole genome into GTA type VLPs. PBSX is a defective prophage that randomly
276 packages 13 Kbp DNA fragments of the *B. subtilis* genome in a GTA-like fashion (Fig. 4c)^{10,33,34}. In
277 contrast to other GTAs it does not transfer the packaged DNA between cells but rather acts similar to a
278 bacteriocin against *B. subtilis* cells that do not carry the PBSX gene cluster¹⁰.

279 DNA sequencing reads derived from purified PBSX particles covered the *B. subtilis* genome unevenly
280 with a maximum 30 fold difference between the lowest and highest covered regions (Fig. 4d). Reads from
281 whole genome sequencing of *B. subtilis* covered the genome evenly slightly increasing toward the origin
282 of replication, as expected³⁵. The genomic region containing PBSX had a lower read coverage in VLP
283 particle derived reads as compared to neighboring genomic regions. This is consistent with results from a
284 previous study where it was found that a genetic marker integrated in the PBSX region was less frequently
285 packaged into particles as compared to a marker in a neighboring region³⁶. Interestingly, the genomic
286 region containing the prophage SPbeta, which gets excised upon mitomycin C treatment³⁷, did not show
287 any higher or lower coverage in the VLP particle derived sequencing reads as compared to neighboring
288 genomic regions (Fig. 4d).

289 Our results show that packaging of host DNA by the GTA-like PBSX element of *B. subtilis* produces a
290 distinct and non-random sequencing coverage pattern that bears similarities to the read coverage pattern
291 produced by the generalized transducing phage P1 (Fig. 3c).

292 **Case study: High occurrence of transduction in the intestinal microbiome**

293 We next assessed the power and application of our transductions approach for detecting transduced
294 DNA in VLPs from complex microbiomes. We sequenced the whole metagenome (~390 mio reads) and
295 VLPs (~360 mio reads) purified from a fecal sample of one mouse to high coverage. We were able to
296 assemble 2143 contigs >40 kbp from the whole metagenome reads with the largest contig being 813 kbp
297 (ENA accession for assembly: ERZ1273841). We discarded contigs <40 kbp because detection of
298 transduction patterns requires coverage analysis of a sufficiently large genomic region. We mapped the
299 metagenomic and VLP reads to the contigs >40 kbp to obtain the read coverage patterns. Of the 2143
300 contigs, 1957 showed a “standard” read coverage pattern (Fig. 5a, Suppl. Table S1), i.e. high even
301 coverage of the contigs with metagenomic reads and low even or no coverage with VLP reads, indicating
302 no mobilization of host DNA in VLPs. The remaining 186 contigs (8.6% of all contigs >40 kbp) showed a
303 read coverage pattern that indicates potential mobilization of DNA in VLPs (Fig. 5b-f, Suppl. Table S1).

304 We classified all contigs taxonomically using CAT³⁸ (Suppl. Tables S2 and S3). The majority of contigs
305 were classified as Bacteroidetes (all contigs: 805, transduction pattern contigs: 83), Firmicutes (all: 586,
306 transduction pattern: 42), Proteobacteria (all: 89, transduction pattern: 3), or not classified at the phylum
307 level (all: 527, transduction pattern: 34). We found that with a few exceptions the relative abundance of
308 contigs assigned to specific phyla was similar between the set of all contigs >40 kbp and the subset of
309 contigs with transduction patterns. The phyla that differed in relative contig abundance were
310 Proteobacteria with less than half the relative abundance in the contigs with transduction patterns,
311 Verrucomicrobia with 3.5x and *Candidatus* Saccharibacteria with 11.5x the contig abundance in the
312 contigs with transduction patterns. Since members of *Cand. Saccharibacteria* have been shown to be
313 extremely small (200 to 300 nm)³⁹ it is likely that they share similar properties with bacteriophages in
314 terms of size and density and thus might get enriched in the VLP fraction. In fact, all transduction patterns
315 *Cand. Saccharibacteria* contigs with a pattern were classified as “unknown” or “unknown, potentially a
316 small bacterium” prior to knowing the taxonomic identity of the contigs.

317 We classified the type of DNA mobilization/transduction in the 186 contigs with a mobilization pattern
318 based on the visual characteristics of the mobilized region in the VLP read coverage, as well as based on
319 annotated genes within the mobilized region. For example, we classified mobilization patterns as prophage
320 if the characteristic pattern showed high coverage with sharp edges on both sides (compare Fig. 2) and the
321 presence of characteristic phage genes (e.g. capsid proteins) as an additional but not required criterion.

322 We observed 74 contigs that indicated induced prophages. Of these, 12 (16%) prophages showed
323 indications of specialized transduction i.e. read coverage above the base level of the contig in regions
324 adjacent to the prophage (Fig. 5b and d). Additionally, we classified 8 patterns as potential prophages or

325 chromosomal islands, as they showed the same pattern as other prophages, but we were unable to find
326 recognizable phage genes in the annotations.

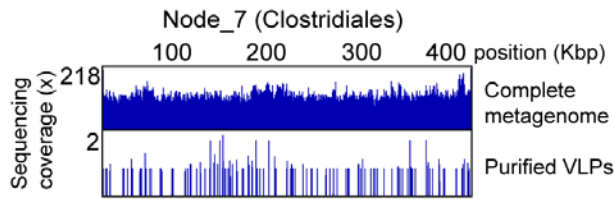
327 We found patterns of potential generalized transduction or GTA carried DNA in 46 contigs, however,
328 some patterns were observed for shorter contigs and could thus potentially be incorrect classifications
329 (Fig. 5c). One of the contigs (NODE_5, classified as Bacteria) with a generalized transduction or GTA
330 pattern additionally showed a sharp coverage drop in a ~15 kbp region only in the VLP reads (Fig. 5c).
331 This region is flanked by a tRNA gene and carries one gene annotated as a potential virulence factor,
332 internalin used by *Listeria monocytogenes* for host cell entry⁴⁰. This region might represent a
333 chromosomal island that was excised from the bacterial chromosome prior to or during production of the
334 unknown VLP and that did not get encapsulated in the VLP. Alternatively, similar strains might be present
335 in the sample, but only some carry the chromosomal island and strains carrying the chromosomal island
336 are less prone to producing the VLPs, e.g., by superinfection resistance provided by the chromosomal
337 island against a generalized transducing phage.

338 We observed 9 patterns that showed strong differences between whole metagenome read coverage and
339 VLP read coverage, but that did not correspond to any of the patterns we analyzed in our proof-of-
340 principle work. However, based on gene annotations we determined that these patterns likely represent
341 retrotransposons or other transposable elements. For example, on contig NODE_1640 (classified as
342 Bacteria by CAT) we observed high coverage with VLP reads on one part of the contig, which carries a
343 gene annotated as a retrotransposon (Fig. 5e). Interestingly, the retrotransposon region is flanked by a *ltrA*
344 gene which is encoded on bacterial group II intron and encodes maturase, an enzyme with reverse
345 transcriptase and endonuclease activity⁴¹. Surprisingly the region containing the *ltrA* gene had above
346 average coverage in the whole metagenome reads, but no coverage in the VLP reads. This suggests that
347 the intron actively reverse splices into expressed RNA with subsequent formation of cDNA⁴¹ leading to
348 increased copy number of this genomic region. As another example, on contig NODE_1223 (classified as
349 Bacteria by CAT) a region containing a transposase gene is strongly overrepresented in the VLP reads
350 suggesting that this region is a transposable element that is packaged into a VLP (Fig. 5e).

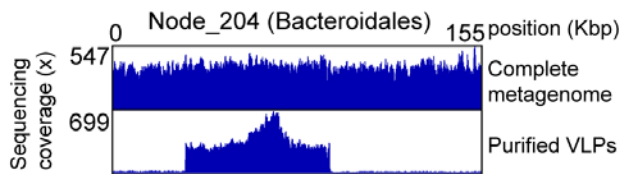
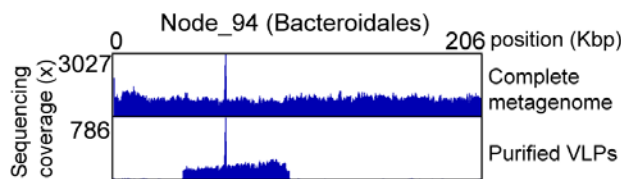
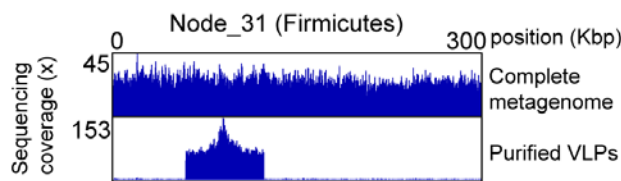
351 Finally, we determined that two patterns are likely lytic phages and 47 patterns are classified as
352 “unknown” transduced DNA, as the coverage pattern is uneven indicating transport in VLPs but we could
353 not determine the type of transport. To provide two examples: (1) in contig NODE_326 (classified as
354 Bacteroidales by CAT) we observed a “hill-like” coverage pattern in the VLP reads for a region of ~30
355 kbp flanked by a tRNA gene (Fig. 5f); and (2) in contig NODE_646 (classified as Clostridiales by CAT)
356 we observed a potential prophage pattern in which we found some of the main phage relevant genes such

357 as major capsid protein, however, within the prophage pattern we observed high coverage spikes for
 358 which we currently have no good explanation.

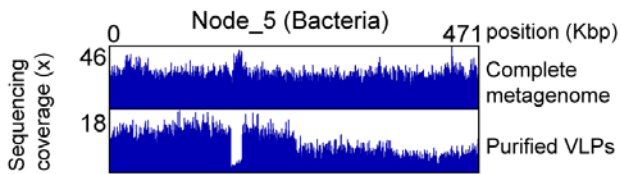
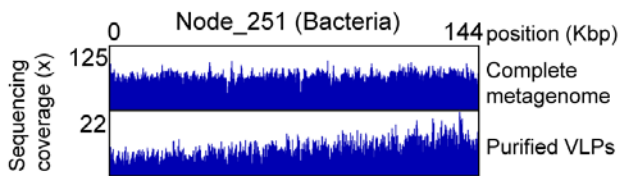
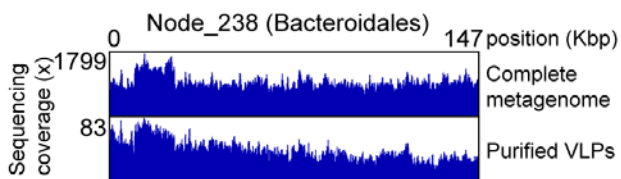
a) Example of a contig without transduction pattern



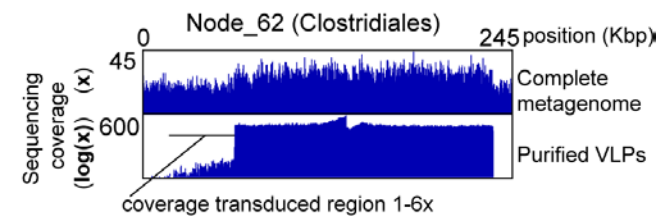
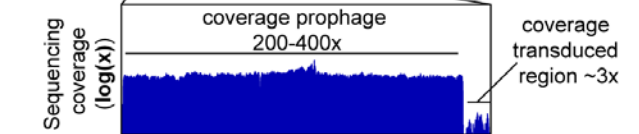
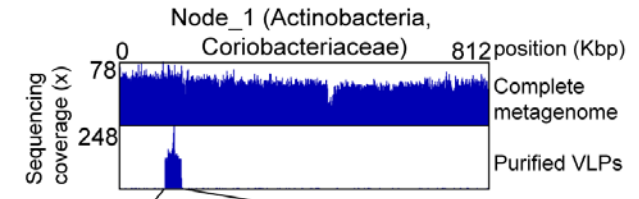
b) Contigs with induced prophages



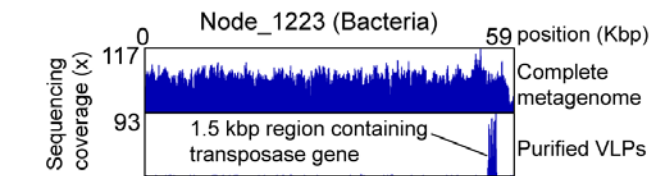
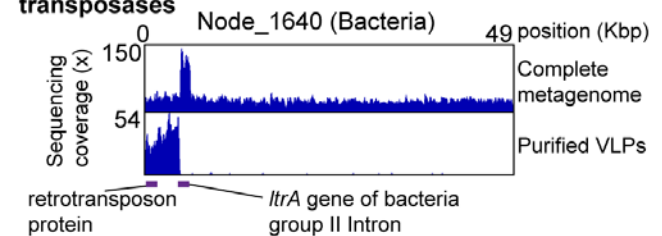
c) Contigs with generalized transduction or GTA pattern



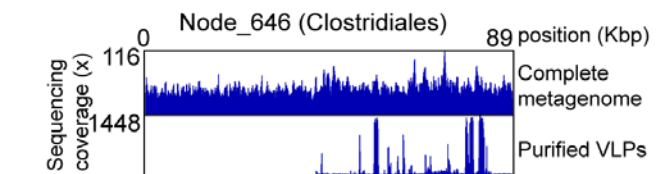
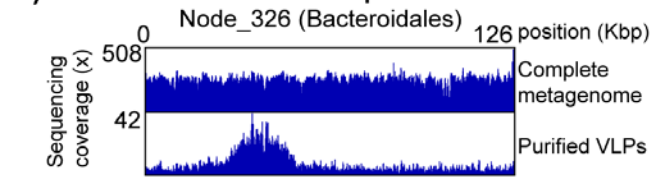
d) Contigs with specialized transduction pattern



e) Patterns associated with retrotransposons and transposases



f) Unknown transduced DNA patterns



359

360 **Figure 5: Example of transduction patterns in the mouse intestinal microbiome.** The taxonomic
361 classification for each contig specified in parentheses after each contig name is the lowest taxonomic level
362 successfully classified by CAT³⁸(Suppl. Table S2)

363 **Conclusions and Outlook**

364 The transductomics approach that we developed should be applicable to a broad range of environments
365 ranging from host-associated microbiomes to soils and aqueous environments. For some environments
366 such as open ocean water samples the approach would need only minor modifications. For example,
367 concentration of VLPs by tangential flow filtration prior to density gradient centrifugation using well
368 established protocols¹⁹. Thus this approach will allow addressing key questions about microbial evolution
369 via HGT in a diversity of microbial communities, including what kind of genes and with what frequency
370 are transduced by VLPs. Among these questions, one of the most pressing ones is what the role of
371 transducing particles is in the transfer of antibiotic resistance genes, which is a topic of current debate⁴²⁻⁴⁵.
372 Apart from its application in studying transduction in microbial communities this approach can also be
373 used to increase our understanding of the molecular mechanisms of different transduction mechanisms by
374 careful analysis of read coverage data from pure cultures that shows exact transduction frequencies of
375 each genomic location without tedious analysis of multiple genomic markers. Mechanisms that can be
376 analyzed include, for example, the identification of *pac* sites in generalized transducers, the size range of
377 transduced genomic loci in specialized transducers, and the analysis of how random DNA packaging by
378 GTAs really is.

379 One of the major surprises for us when analyzing the mouse intestinal transductome data was that around
380 one quarter of the transduction patterns that we identified are unknown. These patterns showed even
381 coverage in the whole metagenome reads and strong uneven coverage in the VLP reads (e.g. Fig. 4e),
382 however, we were unable to associate them clearly with any of transduction modes that we have
383 investigated with pure cultures. We foresee two types of future studies to characterize the nature of the
384 transducing particles that lead to these unknown patterns and to exclude that they are some kind of
385 artifact. First, read coverage patterns of newly discovered modes of transduction have to be analyzed with
386 the “transductomics” approach to correlate the patterns to patterns observed in microbiomes and microbial
387 communities. While we investigated the transduction patterns associated with both major known
388 transduction pathways, as well as more recently discovered transduction pathways, novel modes of
389 transduction are continuously discovered. These novel transduction modes that need to be characterized
390 with our approach include new types of GTAs¹⁰, lateral transduction¹² and DNA transfer in outer
391 membrane vesicles^{46,47}. Second, approaches that allow linking specific transduced DNA sequences to the
392 identity of transducing particles in microbial community samples can be developed. We envision, for
393 example, that high resolution filtration and density gradient based separation of individual VLPs will
394 allow linking the transduced DNA (by sequencing) to the identity of the transducing VLPs using
395 proteomics to identify VLP proteins. Using and developing these approaches further will allow us to
396 increase the range of transduction modes that can be detected in microbial communities, as well as

397 potentially reveal currently unknown types of transduction that are not known from pure culture studies
398 yet.

399 We see several pathways for improving the sensitivity, accuracy and throughput of the transductomics
400 approach in the future. Currently, our ability to detect generalized transduction patterns is limited by the
401 fact that detection of these patterns requires long stretches of the microbial host genome to be assembled.
402 Our P22 and P1 data shows these patterns stretch across genomic regions >500 kbp. Additionally, high
403 sequencing coverage is needed for the detection of these patterns. Assembly of long contigs in
404 metagenomes of high diversity communities is currently hampered by the relatively short read lengths of
405 sequencers that allow for high coverage. We expect, that increasing read numbers of long-read sequencing
406 technologies such as PacBio and Oxford Nanopore in the future will allow to sequence complex
407 microbiomes to sufficient depth for the assembly of long metagenomic contigs. A combination of long-
408 read sequencing for the whole community metagenomes in combination with a short-read, high-coverage
409 approach for the VLP fraction will in the future provide more sensitive and accurate detection of
410 generalized transduction patterns. In addition to improvements in the realm of long-read sequencing we
411 expect the development of computational tools for the automatic or semi-automatic detection of
412 transduction patterns in read coverage data from paired whole metagenome and VLP metagenome
413 sequencing. Such computational tools will enable the high-throughput detection of transduction patterns in
414 many samples, which is currently limited by the need for visual inspection of patterns.

415 **Online Methods**

416 ***In vitro* bacteriophage propagation and induction of transducing prophages and other** 417 **elements**

418 ***Lambda***. *E. coli* KL740 was inoculated into 300 ml of LB and grown to an OD₆₀₀ of 0.7 at 28°C with
419 aeration. The culture flask was transferred to a 42°C water bath for 10 minutes and then incubated at 42° C
420 for 30 min with shaking. The temperature was reduced to 28° C and cell lysis was allowed to proceed for 2
421 hrs. The remaining cells and debris were removed by centrifugation at 2750 x g for 10 minutes and the
422 phage containing culture fluid was filtered through a 0.45 µm membrane.

423 ***P22***. The data set used to analyze generalized transduction by *Salmonella* phage P22 was taken from a
424 previous study assessing methods for phage particle purification from intestinal contents²⁰. For a detailed
425 description of P22 propagation and purification please refer to our previous publication.

426 ***P1***. Lyophilized phage P1 was purchased from ATCC and resuspended in 1 ml of Lennox broth (LB) at
427 room temperature (RT). 200 µl of the phage suspension was added to 10 ml of mid logarithmic phase
428 (OD₆₀₀ ~0.5) *E. coli* ATCC 25922 and incubated for 3 hrs at 37°C with shaking. The bacteria were pelleted
429 at 2750 x g for 10 min and the culture fluid was filtered through a 0.45 µm syringe filter. 100 µl of
430 stationary phase *E. coli* ATCC 25922 was distributed to 15 separate tubes each containing 200 µl of the
431 P1 culture filtrate. The bacteria/phage mixtures were immediately added to molten LB top agar (0.5%
432 agar), poured over LB agar (1.5% agar) plates and incubated overnight (O/N) at 37°C. 2.5 ml of SM-plus
433 buffer (100 mM NaCl, 50 mM Tris·HCl, 8 mM MgSO₄, 5 mM CaCl₂·6H₂O, pH 7.4) was added to the
434 surface each plate and the top agar was scraped off and pooled. The phages were eluted from the top agar
435 by rotation for 1 hour at RT. The top agar suspension was centrifuged at 2750 x g for 10 min, the
436 supernatant was collected and the top agar was washed once with ~30 ml of SM-plus and incubated at RT
437 for an additional 1 hr. Following the wash step centrifugation was repeated and the resulting supernatant
438 was collected. The phage containing supernatants were combined.

439 ***PBSX***. To induce the prophage-like element PBSX from the *B. subtilis* ATCC 6051 genome, a 100 ml
440 culture of *B. subtilis* was grown in LB at 37°C with shaking to an OD₆₀₀ of ~0.5. Mitomycin C was added
441 at a final concentration of 0.5 µg/ml and the culture was incubated at 37°C for 10 minutes. The culture was
442 centrifuged at 2750 x g for 10 min and the pellet was washed with 50 ml of fresh LB and centrifuged a
443 second time. The cell pellet was resuspended in 100 ml of LB and grown for an additional 3 hrs at 37° C
444 with shaking. The cells and debris were removed by centrifugation and the phage containing culture fluid
445 was filtered through a 0.45 µm membrane.

446 ***Enterococcal prophages.*** *E. faecalis* strain VE14089, a derivative of *E. faecalis* V583 that has been cured
447 of its three endogenous plasmids¹⁵, was subcultured to an OD₆₀₀ of 0.025 in 1 L of pre warmed brain heart
448 infusion broth (BHI) and grown statically at 37°C to an OD₆₀₀ of 0.5. To induce excision of integrated
449 prophages, ciprofloxacin was added to the culture at a final concentration of 2 µg/ml and the bacteria were
450 grown for an additional 4 hrs at 37°C. The bacterial cells and debris were centrifuged at 2750 x g for 10
451 min and the culture fluid was filtered through a 0.45µm membrane.

452 **Purification of phage particles from culture fluid**

453 All phage containing culture fluid was treated with 10 U of DNase and 2.5 U of RNase for 1 hr at RT. 1 M
454 solid NaCl and 10 % wt/vol polyethylene glycol (PEG) 8000 was added and the phages were precipitated
455 O/N on ice at 4°C. The precipitated phages were resuspended in 2 ml of SM-plus and loaded directly onto
456 CsCl step gradients (1.35, 1.5 and 1.7 g/ml fractions) and centrifuged for 16 hrs at 83,000 x g. The phage
457 bands were extracted from the CsCl gradients using a 23-gauge needle and syringe, brought up to 4 ml with
458 SM-plus buffer and loaded onto a 10,000 Da molecular weight cutoff Amicon centrifugal filter (EMD
459 Millipore) to remove excess CsCl. The phages were washed 3 times with ~4 ml of SM-plus and then stored
460 at 4°C.

461 **Isolation of phage and host bacterial DNA from pure cultures**

462 Following CsCl purification of phages and phage-like elements, DNA was isolated by adding 0.5 % SDS,
463 20 mM EDTA (pH=8) and 50 µg/ml Proteinase K (New England Biolabs) and incubating at 56°C for 1
464 hour. Samples were cooled to RT and extracted with an equal volume of phenol:chloroform:isoamyl
465 alcohol. The samples were centrifuged at 12,000 x g for 1 min and the aqueous phase containing the DNA
466 was extracted with an equal volume of chloroform. Following centrifugation at ~16,000 x g for 1 min
467 0.3M NaOAc (pH=7) was added followed by an equal volume of 100% isopropanol to precipitate the
468 DNA. The DNA was pelleted at 12,000 x g for 30 min and washed once with 500 µl of 70% ethanol. The
469 samples were decanted and the pellets were air dried for 10 min and resuspended in 100 µl of sterile
470 water.

471 For the isolation of bacterial genomic DNA, we used the Gentra Puregene Yeast/Bacteria Kit (Qiagen)
472 according to the manufacturer's instructions.

473 **Isolation and purification of bacteria and VLPs from mouse fecal pellets for metagenomic 474 sequencing**

475 The entire colon contents of one male C57BL6/J mouse were added to 1.2 ml of SM-plus buffer and
476 homogenized manually with the handle of a sterile disposable inoculating loop. After homogenization the
477 sample was brought up to 2 ml with SM-plus. One third of the sample volume was added to a fresh tube

478 containing 100 mM EDTA and set aside on ice. This represented the unprocessed whole metagenome
479 sample. The remaining two thirds of the sample volume were used to isolate VLPs.

480 VLPs from the homogenized feces were ultra-purified as described previously²⁰. Briefly, the sample was
481 centrifuged at 2500 x g for 5 min, the supernatant transferred to a clean tube and centrifuged a second time
482 at 5000 x g to pellet any residual bacteria and debris. The supernatant was transferred to a sterile 1 ml syringe
483 and filtered through a 0.45 µm syringe filter. The clarified supernatant was treated with 100 U of DNase
484 and 15 U of RNase for 1 hr at 37°C. The sample was loaded onto a CsCl step gradient (1.35, 1.5 and 1.7
485 g/ml fractions) and centrifuged for 16 hrs at 83,000 x g. The VLPs residing at the interface of the 1.35 and
486 1.5 g/ml fractions were collected (~2 ml) and the CsCl was removed by centrifugal filtration as described
487 above. The purified VLPs were disrupted by the addition of 50 µg/ml proteinase K and 0.5% sodium dodecyl
488 sulfate (SDS) at 56° C for 1 hr. The samples were cooled to room temperature and total DNA was extracted
489 by the addition of an equal volume of phenol:chloroform:isoamyl alcohol. The organic phase was separated
490 by centrifugation at 12,000 x g for 2 minutes and the aqueous phase was extracted with an equal volume of
491 chloroform. The DNA was precipitated by the addition of 0.3 M NaOAc, pH 7, and an equal volume of
492 isopropanol. The DNA pellet was washed once with ice cold 70% ethanol and resuspended in 100 µl of
493 sterile water. The DNA was further cleaned on a MinElute spin column (Qiagen) and eluted into 12 µl of
494 elution buffer (Qiagen).

495 To purify total metagenomic DNA, unclarified fecal homogenate was treated with 5 mg/ml lysozyme for
496 30 min at 37° C. The sample was transferred to 2 ml Lysing Matrix B tubes (MP Biomedical) and bead beat
497 in a Bullet Blender BBX24B (Next Advance) at top speed for 1 min followed by placing on ice for 2 min.
498 This was repeated a total of 4 times. The samples were centrifuged at 12,000 x g for 1 min and the DNA
499 from the supernatant was extracted, precipitated and purified as described above.

500 **DNA Sequencing**

501 The concentration of purified microbial DNA was determined using a Qubit 3.0 fluorometer (Thermo-
502 Fisher). Prior to library preparation total microbial DNA was sheared using a Covaris S2 sonicator with a
503 duty cycle of 10%, intensity setting of 5.0 and a duration of 2 x 60 sec at 4° C. Sequencing libraries were
504 generated using the KAPA HTP library preparation kit KR0426 – v3.13 (KAPA Biosystems) with
505 Illumina TruSeq ligation adapters. Library quality was determined using a 2100 Bioanalyzer system
506 (Agilent). Libraries were size selected and purified in the range of 300-900 bp fragments and subjected to
507 Illumina deep sequencing. For DNA sequencing of pure phage cultures and the *E. coli* KL740 genome we
508 used an Illumina NextSeq 500 desktop sequencer. Illumina HiSeq 2500 v3 Sequencing System in rapid run
509 mode was used to sequence the metagenomes and viromes from the feces of the C57BL6/J mouse. All
510 sequencing was performed in paired end mode acquiring 150 bp reads. Per fragment end the following

511 number of reads were obtained; C57BL/6 mouse feces - 76 M reads for the whole metagenome and 97 M
512 reads for the virome, 45 M reads for phage P1, 21 M reads for lambda phage and 27 M reads for the *E.*
513 *coli* KL740 genome, 29 M reads for phage PBSX and 28 M reads for the enterococcal prophages. For the
514 C57BL/6 mouse microbiome we sequenced an additional 75 bp single-end read run to increase coverage.
515 We obtained 313 M 75 bp reads for the whole metagenome and 262 M 75 bp reads for the virome. All
516 DNA sequencing was performed by the Eugene McDermott Center for Human Growth and Development
517 Next Generation Sequencing Core Facility at the University of Texas Southwestern.

518 **Assembly of mouse fecal metagenome**

519 Read decontamination and trimming of the mouse metagenome 75 and 150 bp reads were performed using
520 the BMap short read aligner²¹ as previously described⁴⁸. Briefly, for decontamination, raw reads were
521 mapped to the internal Illumina control phiX174 (J02482.1), the mouse (mm10) and human (hg38)
522 reference genomes using the bbsplit algorithm with default settings. The resulting unmapped reads were
523 adapter trimmed and low-quality reads and reads of insufficient length were removed using the bbdisk
524 algorithm with the following parameters: ktrim = lr, k = 20, mink = 4, minlength = 20, qtrim = f. The reads
525 were assembled using SPAdes version 3.6.1⁴⁹ with the following parameters: --only-assembler -k
526 21,33,55,77,99. Assembled contigs <40 kbp were discarded. The assembly resulted in 2143 contigs >40
527 kbp.

528 **Taxonomic classification and annotation of metagenomic contigs**

529 The 2143 contigs >40 kbp from the assembly of the mouse fecal metagenome were taxonomically
530 classified using the Contig Annotation Tool (CAT)³⁸ (version 2019-07-19). Genes were predicted and
531 annotated using the automated PROKKA pipeline (v1.11)⁵⁰.

532 **Read mapping and read coverage visualization**

533 The whole (meta)genome and purified VLP read sets were mapped onto the corresponding reference
534 genomes of pure culture organisms or the mouse fecal metagenome contigs using BMap²¹ with the
535 following parameters: ambiguous=random qtrim=lr minid=0.97. The generated read mapping files (.bam)
536 were sorted and indexed using SAMtools⁵¹. Integrative Genomics Viewer (IGV) tools were used to
537 generate tiled data files (.tdf) from the read mapping (.bam) files for data compression and faster access in
538 IGV using the following parameters: count command, zoom levels: 9, using the mean, window size: 25 or
539 100²². Read coverage patterns were displayed and visually assessed in IGV using a linear or if needed log
540 scale.

541 **Data availability**

542 All sequencing read data generated for this study is available from the European Nucleotide Archive
543 (ENA) through study PRJEB33536 (<https://www.ebi.ac.uk/ena/data/view/PRJEB33536>). This data
544 includes the reads for the mouse whole metagenomes and VLP fraction, *E. faecalis* VLPs, *B. subtilis*
545 VLPs, *E. coli* phage P1, *E. coli* phage λ , the whole genome sequencing of *E. coli* KL740 (*E. coli* with
546 lambda phage integrated) and the contigs >40 kbp from the mouse whole metagenome assembly (contig
547 file accession number ERZ1273841).

548 In addition to the de novo generated data we used existing genome assemblies and sequencing read sets
549 for individual bacteria including *Bacillus subtilis* subsp. subtilis str. 168 complete genome from NCBI
550 RefSeq (NC_000964.3), *B. subtilis* 168 genome sequencing read set from the ENA (Study: PRJDB1076,
551 Sample: SAMD00008600), *Enterococcus faecalis* V583 complete genome from NCBI RefSeq
552 (NC_004668.1), *E. faecalis* V583 sequencing read set from the ENA (Study: PRJEB13005, Sample:
553 ERS1085927), *Escherichia coli* K12 complete genome from NCBI RefSeq (NC_000913.3), *E. coli*
554 NCM3722 (*E. coli* K12 with Lambda phage integrated) complete genome sequence from NCBI GenBank
555 (CP011495.1), phage P1 complete genome sequence from NCBI RefSeq (NC_005856.1), *E. coli* K12
556 genome sequencing read set from the ENA (Study: PRJNA251794, Sample: SAMN02840692),
557 *Salmonella enterica* subsp. enterica serovar typhimurium str. LT2 complete genome sequence from NCBI
558 RefSeq (NC_003197.1), *S. typhimurium* LT2 genome sequencing read set from ENA (Study:
559 PRJNA203445, Sample: SAMN02367645), and a read set of CsCl density gradient purified P22 phage
560 (Study: PRJEB6941, Sample: SAME2690949)²⁰.

561 **Author Contributions**

562 M.K. and B.A.D. designed the study. M.K. and B.A.D. performed experiments. M.K. and B.A.D.
563 performed bioinformatic analyses. B.B. developed BBTools and implemented new parameters in BBMap
564 needed for analyses performed in this study. K.S. and L.V.H. provided conceptual input, strains and
565 specialized reagents. M.K. and B.A.D. wrote the paper with input from all authors.

566 **Acknowledgements**

567 We would like to thank Kelly Ruhn for assistance with animals and Vanessa Schmid and Rachel Bruce of
568 the University of Texas Southwestern Medical Center's Next Generation Sequencing Core for assistance
569 with Illumina library construction and sequencing support.

570 This work was supported in part by the USDA National Institute of Food and Agriculture Hatch project
571 1014212 (M.K.), the Foundation for Food and Agriculture Research Grant ID: 593607 (M.K.), the NC
572 State Chancellor's Faculty Excellence Program Cluster on Microbiomes and Complex Microbial
573 Communities (M.K.), National Institutes of Health Grants R01AI141479 (B.A.D.), K01DK102436
574 (B.A.D), and R01DK070855 (L.V.H.), and the Howard Hughes Medical Institute (L.V.H.).

575

576 **Competing Interests**

577 The authors declare no competing interests.

578 **References**

- 579 1. Zhaxybayeva, O. & Doolittle, W. F. Lateral gene transfer. *Curr. Biol.* **21**, R242–R246 (2011).
- 580 2. Soucy, S. M., Huang, J. & Gogarten, J. P. Horizontal gene transfer: building the web of life. *Nat. Rev.*
581 *Genet.* **16**, 472–482 (2015).
- 582 3. Smillie, C. S. *et al.* Ecology drives a global network of gene exchange connecting the human
583 microbiome. *Nature* **480**, 241–244 (2011).
- 584 4. Oladeinde, A. *et al.* Horizontal Gene Transfer and Acquired Antibiotic Resistance in *Salmonella*
585 *enterica* Serovar Heidelberg following In Vitro Incubation in Broiler Ceca. *Appl. Environ. Microbiol.*
586 **85**, (2019).
- 587 5. Borgeaud, S., Metzger, L. C., Scignari, T. & Blokesch, M. The type VI secretion system of *Vibrio*
588 *cholerae* fosters horizontal gene transfer. *Science* **347**, 63–67 (2015).
- 589 6. Chen, J. & Novick, R. P. Phage-mediated intergeneric transfer of toxin genes. *Science* **323**, 139–141
590 (2009).
- 591 7. Hehemann, J.-H. *et al.* Transfer of carbohydrate-active enzymes from marine bacteria to Japanese gut
592 microbiota. *Nature* **464**, 908–912 (2010).
- 593 8. Mongodin, E. F. *et al.* The genome of *Salinibacter ruber*: Convergence and gene exchange among
594 hyperhalophilic bacteria and archaea. *Proc. Natl. Acad. Sci.* **102**, 18147–18152 (2005).
- 595 9. Popa, O., Landan, G. & Dagan, T. Phylogenomic networks reveal limited phylogenetic range of
596 lateral gene transfer by transduction. *ISME J.* **11**, 543–554 (2017).
- 597 10. Lang, A. S., Zhaxybayeva, O. & Beatty, J. T. Gene transfer agents: phage-like elements of genetic
598 exchange. *Nat. Rev. Microbiol.* **10**, 472–482 (2012).
- 599 11. Chiang, Y. N., Penadés, J. R. & Chen, J. Genetic transduction by phages and chromosomal islands:
600 The new and noncanonical. *PLOS Pathog.* **15**, e1007878 (2019).
- 601 12. Chen, J. *et al.* Genome hypermobility by lateral transduction. *Science* **362**, 207–212 (2018).

- 602 13. Thierauf, A., Perez, G. & Maloy, S. Generalized Transduction. in *Bacteriophages: Methods and*
603 *Protocols, Volume 1: Isolation, Characterization, and Interactions* (eds. Clokie, M. R. J. &
604 Kropinski, A. M.) 267–286 (Humana Press, 2009). doi:10.1007/978-1-60327-164-6_23.
- 605 14. Christie, G. E. & Dokland, T. Pirates of the Caudovirales. *Virology* **434**, 210–221 (2012).
- 606 15. Matos, R. C. *et al.* Enterococcus faecalis Prophage Dynamics and Contributions to Pathogenic Traits.
607 *PLOS Genet.* **9**, e1003539 (2013).
- 608 16. Jiang, S. C. & Paul, J. H. Gene Transfer by Transduction in the Marine Environment. *Appl. Environ.*
609 *Microbiol.* **64**, 2780–2787 (1998).
- 610 17. Kenzaka, T., Tani, K. & Nasu, M. High-frequency phage-mediated gene transfer in freshwater
611 environments determined at single-cell level. *ISME J.* **4**, 648–659 (2010).
- 612 18. Sander, M. & Schmieger, H. Method for host-Independent detection of generalized transducing
613 bacteriophages in natural habitats. *Appl. Environ. Microbiol.* **67**, 1490–1493 (2001).
- 614 19. Thurber, R. V., Haynes, M., Breitbart, M., Wegley, L. & Rohwer, F. Laboratory procedures to
615 generate viral metagenomes. *Nat. Protoc.* **4**, 470–483 (2009).
- 616 20. Kleiner, M., Hooper, L. V. & Duerkop, B. A. Evaluation of methods to purify virus-like particles for
617 metagenomic sequencing of intestinal viromes. *BMC Genomics* **16**, 7 (2015).
- 618 21. Bushnell, B. BBMap. *SourceForge* <https://sourceforge.net/projects/bbmap/>.
- 619 22. Thorvaldsdóttir, H., Robinson, J. T. & Mesirov, J. P. Integrative Genomics Viewer (IGV): high-
620 performance genomics data visualization and exploration. *Brief. Bioinform.* **14**, 178–192 (2013).
- 621 23. Gottesman, M. E. & Weisberg, R. A. Little Lambda, who made thee? *Microbiol. Mol. Biol. Rev.* **68**,
622 796–813 (2004).
- 623 24. Morse, M. L., Lederberg, E. M. & Lederberg, J. Transduction in Escherichia Coli K-12. *Genetics* **41**,
624 142–156 (1956).
- 625 25. Ebel-Tsipis, J., Botstein, D. & Fox, M. S. Generalized transduction by phage P22 in Salmonella
626 typhimurium: I. Molecular origin of transducing DNA. *J. Mol. Biol.* **71**, 433–448 (1972).

- 627 26. Schmieger, H. Packaging signals for phage P22 on the chromosome of *Salmonella typhimurium*. *Mol.*
628 *Gen. Genet. MGG* **187**, 516–518 (1982).
- 629 27. Casjens, S. & Hayden, M. Analysis in vivo of bacteriophage P22 headful nuclease. *J. Mol. Biol.* **199**,
630 467–474 (1988).
- 631 28. Hanks, M. C., Newman, B., Oliver, I. R. & Masters, M. Packaging of transducing DNA by
632 bacteriophage P1. *Mol. Gen. Genet. MGG* **214**, 523–532 (1988).
- 633 29. Masters, M. Generalized Transduction. in *Escherichia coli and Salmonella: Cellular and Molecular*
634 *Biology* 2421–441 (American Society for Microbiology, 1996).
- 635 30. José R. Penadés & Gail E. Christie. The phage-inducible chromosomal islands: A family of highly
636 evolved molecular parasites. *Annu. Rev. Virol.* **2**, 181–201 (2015).
- 637 31. Duerkop, B. A., Clements, C. V., Rollins, D., Rodrigues, J. L. M. & Hooper, L. V. A composite
638 bacteriophage alters colonization by an intestinal commensal bacterium. *Proc. Natl. Acad. Sci.* **109**,
639 17621–17626 (2012).
- 640 32. Kunst, F. *et al.* The complete genome sequence of the Gram-positive bacterium *Bacillus subtilis*.
641 *Nature* **390**, 249–256 (1997).
- 642 33. Wood, H. E., Dawson, M. T., Devine, K. M. & McConnell, D. J. Characterization of PBSX, a
643 defective prophage of *Bacillus subtilis*. *J. Bacteriol.* **172**, 2667 (1990).
- 644 34. Canchaya, C., Fournous, G., Chibani-Chennoufi, S., Dillmann, M.-L. & Brüssow, H. Phage as agents
645 of lateral gene transfer. *Curr. Opin. Microbiol.* **6**, 417–424 (2003).
- 646 35. Korem, T. *et al.* Growth dynamics of gut microbiota in health and disease inferred from single
647 metagenomic samples. *Science* **349**, 1101 (2015).
- 648 36. Anderson, L. M. & Bott, K. F. DNA packaging by the *Bacillus subtilis* defective bacteriophage
649 PBSX. *J. Virol.* **54**, 773 (1985).
- 650 37. Abe, K. *et al.* Developmentally-Regulated Excision of the SP β Prophage Reconstitutes a Gene
651 Required for Spore Envelope Maturation in *Bacillus subtilis*. *PLOS Genet.* **10**, e1004636 (2014).

- 652 38. von Meijenfeldt, F. A. B., Arkhipova, K., Cambuy, D. D., Coutinho, F. H. & Dutilh, B. E. Robust
653 taxonomic classification of uncharted microbial sequences and bins with CAT and BAT. *Genome*
654 *Biol.* **20**, 217 (2019).
- 655 39. He, X. *et al.* Cultivation of a human-associated TM7 phylotype reveals a reduced genome and
656 epibiotic parasitic lifestyle. *Proc. Natl. Acad. Sci.* **112**, 244–249 (2015).
- 657 40. Bonazzi, M., Lecuit, M. & Cossart, P. *Listeria monocytogenes* Internalin and E-cadherin: From Bench
658 to Bedside. *Cold Spring Harb. Perspect. Biol.* **1**, (2009).
- 659 41. Cousineau, B., Lawrence, S., Smith, D. & Belfort, M. Retrotransposition of a bacterial group II intron.
660 *Nature* **404**, 1018–1021 (2000).
- 661 42. Haaber, J. *et al.* Bacterial viruses enable their host to acquire antibiotic resistance genes from
662 neighbouring cells. *Nat. Commun.* **7**, 1–8 (2016).
- 663 43. Enault, F. *et al.* Phages rarely encode antibiotic resistance genes: a cautionary tale for virome
664 analyses. *ISME J.* **11**, 237–247 (2017).
- 665 44. Modi, S. R., Lee, H. H., Spina, C. S. & Collins, J. J. Antibiotic treatment expands the resistance
666 reservoir and ecological network of the phage metagenome. *Nature* **499**, 219–222 (2013).
- 667 45. Calero-Cáceres, W., Ye, M. & Balcázar, J. L. Bacteriophages as Environmental Reservoirs of
668 Antibiotic Resistance. *Trends Microbiol.* **27**, 570–577 (2019).
- 669 46. Bitto, N. J. *et al.* Bacterial membrane vesicles transport their DNA cargo into host cells. *Sci. Rep.* **7**,
670 1–11 (2017).
- 671 47. Fulsundar, S. *et al.* Gene Transfer Potential of Outer Membrane Vesicles of *Acinetobacter baylyi* and
672 Effects of Stress on Vesiculation. *Appl. Environ. Microbiol.* **80**, 3469–3483 (2014).
- 673 48. Duerkop, B. A. *et al.* Murine colitis reveals a disease-associated bacteriophage community. *Nat.*
674 *Microbiol.* **3**, 1023–1031 (2018).
- 675 49. Bankevich, A. *et al.* SPAdes: a new genome assembly algorithm and its applications to single-cell
676 sequencing. *J. Comput. Biol.* **19**, 455–477 (2012).
- 677 50. Seemann, T. Prokka: rapid prokaryotic genome annotation. *Bioinformatics* **30**, 2068–2069 (2014).

678 51. Li, H. *et al.* The Sequence Alignment/Map format and SAMtools. *Bioinformatics* **25**, 2078–2079
679 (2009).
680